The influence of finer fraction and size-ratio on the micro-scale properties of dense bimodal materials

The influence of finer fraction and size-ratio on the micro-scale properties of dense bimodal materials

T. Shire*, C. O'Sullivan and K. Hanley

Department of Civil and Environmental Engineering, Imperial College London, UK

*: thomas.shire09@imperial.ac.uk

This is an author generated postprint of the article:

Shire, T., O'Sullivan, C., & Hanley, K. (2014b). The influence of finer fraction and size-ratio on the micro-scale properties of dense bimodal materials. In: *Proceedings of the International Symposium on Geomechanics from Micro to Macro*, *Cambridge, UK, September 2014,* CRC Press

ABSTRACT

The properties of cohesionless bimodal materials are known to be influenced by the volumetric fraction of finer particles, F_{fine}, and the size ratio, $\chi = D_{coarse}/D_{fine}$. Two aspects of this are: *(i)* an increase in χ will lead to finer particles packing more efficiently between the larger particles; *(ii)* there is a critical value of F_{fine} between 24 and 29% at which the finer particles will just fill the voids between the larger particles. Motivated by an interest in developing a comprehensive understanding of the mechanics of internal erosion of dam filters, in this paper Discrete Element Modeling (DEM) simulations are carried out on bimodal samples of spheres with χ of 2, 4, 6, 8 and 10 and F_{fine} of 20, 25, 30 and 35% by volume. Each sample is isotropically compressed to a very dense state and the number of particles in the simulations ranged from 307 to 54033. The number and magnitude of contacts between particles of the same and of different sizes is considered to give an insight into how F_{fine} and χ can affect the stress transfer characteristics of bimodal materials. In particular it is shown that for $F_{fine} \geq 30\%$ fine and large particles contribute approximately equally to stress transfer, whereas for materials with $F_{fine} \leq 25\%$, an increase in χ is shown to reduce the contribution of the finer particles significantly. These findings can be linked to earlier experimental observations considering filter stability (Skempton and Brogan, 1994), but also give insight into the sensitivity of other mechanical properties to the finer fraction and the size ratio (e.g. effect on void ratio and position of the critical state line (Rahman et al., 2008)).

1 INTRODUCTION

Most soil mechanics theory for cohesionless soils has been developed from experiments using uniformly graded or “clean” sands. However, the addition of cohesionless fines to create gap-graded or bimodal soils is known to influence soil properties. Two examples of this are *(i)* internal stability and *(ii)* the position of the critical state line (CSL)

This paper analyses the effect of varying the volumetric proportion of fines F_{fine}, and the size-ratio between coarse and fine fraction, $\chi = D_{coarse}/D_{fine}$ on the micro-scale properties of homogeneous, isotropic collections of bimodal spheres using micro-scale discrete element modeling (DEM) (Cundall & Strack, 1979). The proportion of the overall effective stress transferred through the fines is emphasized.

1.1 *Internal instability*

Internal stability describes the ability of the coarse fraction of a soil to prevent the erosion of the fines under seepage. Internally unstable soils are typically broadly or gap-graded and cohesionless (ICOLD, 2013).

Kenney and Lau (1985) defined three prerequisites for internal instability: *(i)* a primary fabric of coarse particles which transfers stresses; *(ii)* loose particles present in the voids between the primary fabric, which do not carry effective stress and can be moved by seepage; *(iii)* the inter-void constrictions within the primary fabric must be large enough to allow the loose particles to be transported from void to void by seepage. Skempton and Brogan (1994), found that internal instability can initiate at lower hydraulic gradients than would be expected to cause failure by heave. Skempton and Brogan concluded that this was due to the loose fines between the primary matrix carrying reduced effective stress. They proposed to quantify this effect using a stress-reduction factor, α, defined as the effective stress in the fines compared to the overall effective stress:

$$\sigma'_{\text{fine}} = \alpha\sigma' \qquad (1)$$

where σ'_{fine} is the effective stress transferred by the finer fraction and σ' is effective overburden stress.

Combining the stress-reduction factor with Terzaghi’s theory for heave at zero effective stress, the critical hydraulic gradient for a cohesionless soil with no surface loading becomes:

$$i_c = \alpha \frac{\gamma'}{\gamma_w} \qquad (2)$$

Where i_c is the critical hydraulic gradient for internal instability; γ' is the buoyant unit weight; γ_w is the unit weight of water. Note that when α = 1, the soil is internally stable and Equation 2 becomes the Terzaghi relationship. Li and Fannin (2012) derived a generalized form of Equation 2 for the case where an applied stress is acting on the internally unstable layer.

Skempton and Brogan (1994) identified two key fines contents:

(i) the critical fines content, S*, at which the fines just fill the voids between the coarse particles, and below which $\alpha < 1$. S* was estimated to fall between F_{fine} = 24% and 29% for dense and loose samples respectively.

(ii) the fines content at which the fines completely separate the coarse particles from one another, S_{max}, which Skempton and Brogan (1994) stated should be no higher than F_{fine} = 35%.

When $F_{fine} < S^*$ the soil has an "underfilled" fabric, when $S^* < F_{fine} < S_{max}$ "filled" and $F_{fine} > S_{max}$ "overfilled", as shown schematically in Figure 1. Shire et al. (2014) modeled a series of samples with PSDs matching soils with a range of internal stability using discrete element modeling (DEM).

They calculated α directly, and α was found depend on F_{fine}, relative density, and the empirical Kézdi (1979) criterion for internal instability, which gives a measure of size-ratio between the coarse and fine particles. Shire and O'Sullivan (2013) also showed that there is a link between Kézdi and micro-scale parameters such as coordination number.

1.2 *Load:deformation response*

Reliable determination of the CSL is important in predicting the shear behavior of sands e.g. for the determination of the state parameter (Been and Jeffries, 1985). However, the addition of cohesionless fines to a sand has been shown to lower the position of the CSL in e-ln(p′) space up to a threshold value of $F_{fine} \approx 25\%$. Once this threshold value has been reached, further addition of fines is found to raise the position of the CSL (Thevanayagam et al., 2002, Ni et al., 2004). Thevanayagam et al. (2002) proposed that this behavior was due to the fines playing a disproportionately small role in shear resistance.

Thevanayagam et al. (2002) hypothesized that five cases to describe the evolution of sandy soil fabric with increasing cohesionless fines content exist:

(i) finer particles are fully confined within voids between coarse particles and provide no support to the coarse particles;

(ii) finer particles are partially in contact with and provide some support to coarse particles;

(iii) most finer particles are confined within voids but some finer particles separate coarse particles from one another, increasing the fragility of the soil;

(iv-1) coarse and fine particles both contribute towards shear strength;

(iv-2) coarse particles are fully dispersed within a matrix of finer particles, which control shear strength.

Cases (i) to (iii) refer to $F_{fine} < S^*$, whereas (iv-1) and (iv-2) refer to $F_{fine} > S^*$.

Thevanayagam et al. (2002), following Mitchell (1976), also proposed that for $F_{fine} < S^*$ the equivalent granular void ratio e* should be used in place of void ratio, e, as a state variable with which to determine the CSL for a given sand, regardless of fines content, where:

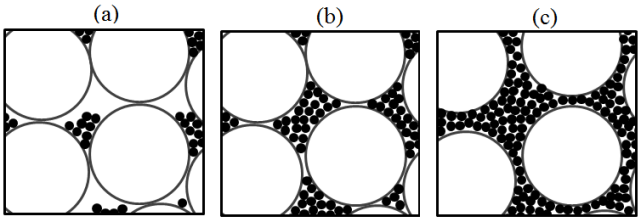

Figure 1. Evolution of fabric with fines content: (a) underfilled; (b) filled; (c) overfilled

$$e^* = \frac{e + (1-b)F_{fine}}{1 - (1-b)F_{fine}} \qquad (3)$$

where b is the proportion of fines which contribute to shear resistance. Rahman et al. (2008) proposed that the parameter b is related to both F_{fine} and the size-ratio, χ and presented a semi-empirical relationship.

2 MODELING

2.1 *Simulation approach and samples analyzed*

DEM simulations were carried out using the open source code Granular LAMMPS (Plimpton, 1995). Samples were created by generating a cloud of non-contacting frictionless spheres with random locations within a periodic cell. The samples were compressed isotropically and monotonically to a mean normal stress p′ = 50 kPa. A servo-controlled algorithm was used to adjust the strain rate until the target stress was reached (Thornton and Antony, 1998). This approach generates samples with the densest possible packing at this stress level.

Simulations were terminated once p′ and the coordination number were both steady for 20,000 timesteps. All the results presented here correspond to this end state. The simulations have all been carried out in a gravity free-environment, to allow the use of a periodic cell and to allow easy identification of those particles which participate in effective stress transfer through the sample. Further details of the simulation methodology are given in Shire (2014).

A total of 20 simulations were carried out using bimodal samples (i.e. containing particles of just two discrete diameters), which were formed from combinations of F_{fine} = 20, 25, 30 and 35% and χ = 2, 4, 6, 8 and 10. In each sample there were 100 coarse particles, with the

equivalent fine particles placed to match F_{fine}. The total number of particles in the simulations ranged from 307 to 54033.

2.2 *Calculation of α*

In equations (1) and (2), α is an indirect measure of the stress in the fines, inferred from macro-scale observations in laboratory tests. The DEM simulations data enable direct calculation of α. In a DEM model the smallest volume over which stress can be quantified is a single particle and here the average stress tensor within a particle, $\overline{\sigma}_{ij}^{p}$, was determined using the approach described in Potyondy and Cundall (2004). The mean particle stress is then $p^{p} = (1/3)\overline{\sigma}^{p}{}_{ii}$.

An isotropic stress state is considered here, and so α is defined in terms of the mean (effective) normal stress p′, which for the whole sample is:

$$p' = \frac{1}{V}\sum_{p=1}^{N_p}(p^{p}V^{p}) \tag{4}$$

where V^{p} is particle volume and N_p is the number of particles. The mean normal stress for the finer fraction is:

$$p'_{fine} = \frac{(1-n)}{\sum_{Np,\,fine} V^{p}}\sum_{p=1}^{Np,\,fine}(p^{p}V^{p}) \tag{5}$$

where: *n*: sample porosity; $N_{p,fine}$: number of fine particles. The stress-reduction in the finer fraction is then:

$$\alpha = p'_{fine} / p' \tag{6}$$

3 RESULTS

3.1 *Verification of DEM model*

McGeary (1961) carried out experiments on bimodal mixtures of glass spheres to investigate the maximum densities that could be obtained; the data from these experiments was considered by Lade et al. (1998). The DEM and experimental data are compared in Figure 2, which illustrates the variation in e_{min}, the minimum void ratio for a given χ value for frictionless simulations (i.e. α=0).

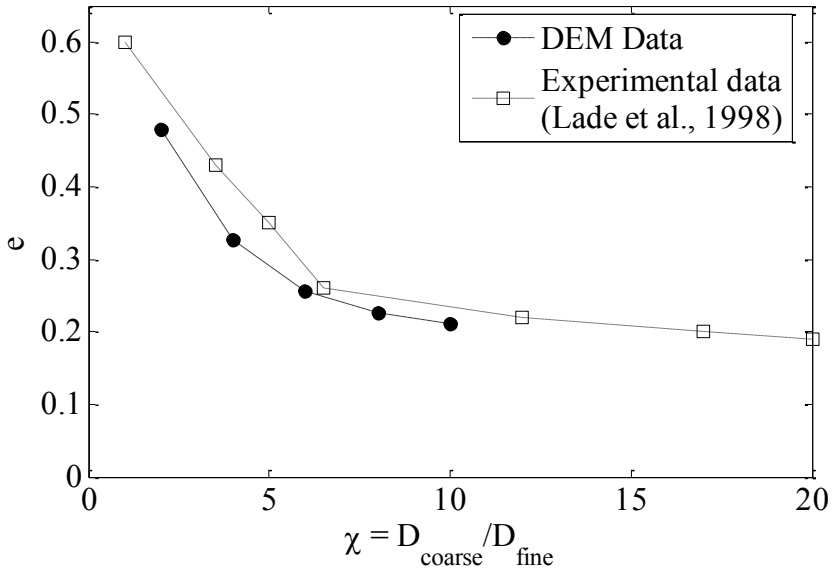

Figure 2. Variation of minimum void ratio with size ratio

There is good agreement between the simulations and experiments, although the DEM data give a slightly denser packing at a given χ. This observed difference is to be expected as the DEM particles are perfectly spherical and frictionless; physical ballotini always deviate from this ideal. As χ increases the rate at which e_{min} decreases reduces; the reduction is gradual (smooth) for the DEM data, however the experiments exhibit a distinct change in rate at around χ = 7. As illustrated schematically in Figure 3, Lade et al. concluded that the variation in e_{min} occurs because the fines pack more efficiently between the coarse particles when the size ratio increases. Lade et al. hypothesized that beyond χ = 7 the fines are fully able to fit within the voids between coarse particles, thus explaining the change in slope observed in Figure 2.

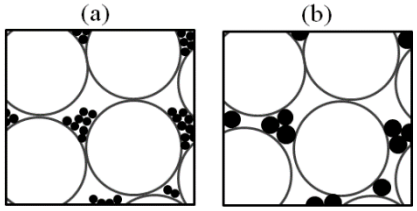

Figure 3. Evolution of fabric with size-ratio: (a) large ratio, fines fit efficiently in voids; (b) small ratio, fines mismatch with voids

3.2 *Relationship between F_{fine}, χ and void ratio*

In Figure 4 the relationship between F_{fine} and e is presented for each χ value in the DEM simulations. For the F_{fine} values presented here there is little overall variation of e with F_{fine} for a given size ratio, however the F_{fine} at which e_{min} is obtained decreases with increasing χ.

At F_{fine} = 20% the values of e_{min} do not vary for 6 < χ < 10, possibly because at this F_{fine} value the fines completely fit between the coarse particles, and therefore e_{min} is dependent on the densest packing which can be achieved by the coarse particles. As χ reduces from χ = 6 to χ = 2, e increases. This may be because the fines are no longer able to fully fit between the coarse particles as shown schematically in Figure 3, so e_{min} is no longer dependent solely on the densest arrangement of the coarse particles.

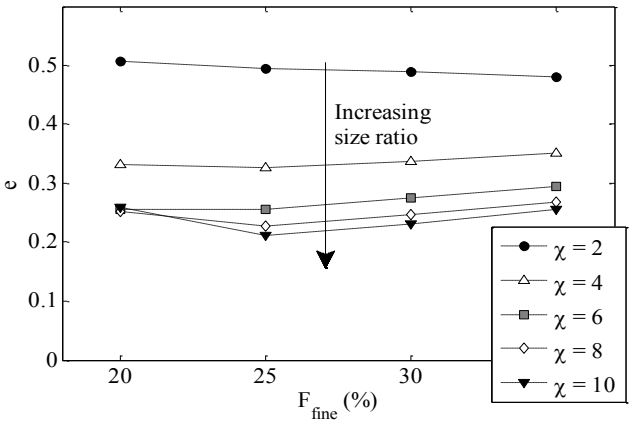

Figure 4. Variation of void ratio with F_{fine} and χ

3.3 *Micro-scale properties of bimodal materials*

A simple scalar measure of soil fabric is the coordination number, Z:

$$Z = 2N_c / N_p \quad (7)$$

where N_c is the number of interparticle contacts in the system.

Figure 5 shows the variation of Z with χ for each of the samples. For F_{fine} = 20% there is a steep reduction from Z = 5.04 at χ = 2 to Z = 0.17 at χ = 6. Z < 1 is possible as gravity has been neglected. In a bimodal material the fine particles dominate numerically, even when accounting for only a fraction of the total volume (when χ = 10, one coarse particle has the same volume as 1000 fines). This means that the coordination number is largely determined by contacts involving the fines. The reduction of Z between χ = 2 and χ = 6 for the F_{fine} = 20% material is evidence that the fines transition from being well connected to being predominantly unconnected and non-stress transmitting. This supports the argument of Lade et al. (1998) that as χ increases fines are better able to fit within voids and so play a reduced role in stress transfer.

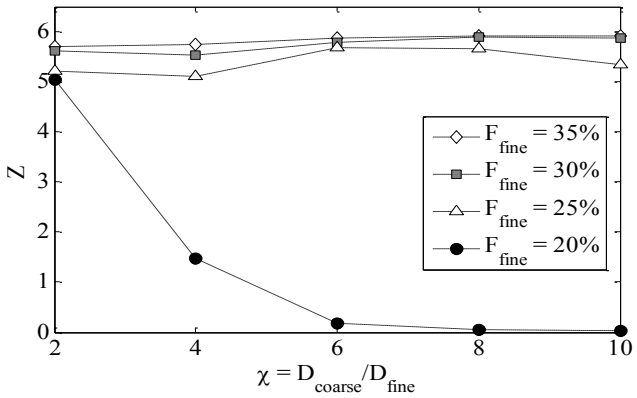

Figure 5. Variation of coordination number with size ratio

For $F_{fine} \geq 25\%$ there is little variation of Z with χ. This is because the fines completely fill the voids between the coarse particles and so have many interparticle contacts, regardless of F_{fine} or χ. This confirms the hypothesis of Skempton and Brogan (1994) that for materials at their highest relative density fines fill voids between coarse particles at $F_{fine} \approx 24\%$.

Further insight into the role of coarse and fine particles in the fabric of bimodal materials can be gained through the use of partial coordination numbers (e.g. Minh and Cheng, 2013):

$$Z^{fine} = 2(N_{c,fine\text{-}fine} + N_{c,fine\text{-}coarse}) \quad / N_{p,fine} \tag{8}$$

$$Z^{coarse} = 2(N_{c,coarse\text{-}coarse} + N_{c,fine\text{-}coarse}) \quad / N_{p,coarse} \tag{9}$$

$$Z^{coarse\text{-}coarse} = 2(N_{c,coarse\text{-}coarse}) \quad / N_{p,coarse} \tag{10}$$

Where Z^{fine}, Z^{coarse} and $Z^{coarse\text{-}coarse}$ are the fine, coarse, and coarse to coarse coordination numbers and $N_{c,fine\text{-}coarse}$ is the number of contacts between coarse and fine particles, etc.

Figure 6(a) shows the variation of Z^{fine} with χ; this is very similar to the variation of Z with χ (Figure 5). Figure 6(b) shows the variation of Z^{coarse} with χ.

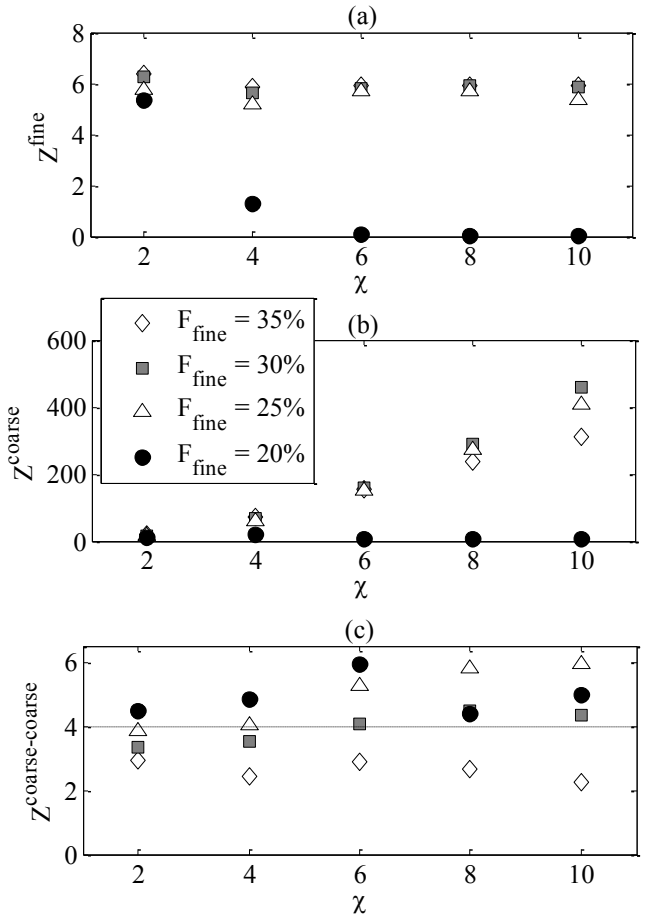

Figure 6: Variation with size ratio of: (a) fine coordination number; (b) coarse coordination number; (c) coarse-coarse coordination number

For $F_{fine} \geq 25\%$, Z^{coarse} increases with χ. For $\chi = 10$ the coarse particles have several hundred contacts per particle, due to the large number of fines which can make contact with each coarse particle.

Samples with $\chi \geq 6$ and $F_{fine} = 20\%$ fall below the Skempton and Brogan S* limit defined above., These samples have a stable primary matrix of interconnected coarse particles, between which are poorly connected, non-stress transmitting fines and so Z^{fine} is small and $Z^{coarse\text{-}coarse}$ is large.

All the samples with $F_{fine} = 35\%$ and those with $\chi \leq 4$ and $F_{fine} = 30\%$ fall above the Skempton and Brogan S_{max} (also defined above). Here, $Z^{coarse\text{-}coarse} < 4$ as the coarse particles are separated from one another; $Z^{coarse\text{-}coarse} = 4$ is highlighted, as this represents the minimum number of contacts between coarse particles required to form a self-supporting, stress transmitting "coarse matrix".

The remaining samples fall between S* and S_{max}. $Z^{coarse\text{-}coarse} > 4$ meaning that a coarse matrix can form. However, as $Z^{fine} > 4$, the fines also form part of the stress transmitting matrix as they fill the voids between the coarse particles.

3.4 *Distribution of stress within bimodal materials*

Figure 7 shows the variation of α with χ and F_{fine}. When the stress in the fines is higher than the overall mean stress $\alpha > 1$. In samples with $F_{fine} \geq 30\%$, $\alpha \approx 1$, indicating that the coarse and fine particles contribute approximately equally to stress transfer . The same is true of samples with $\chi = 2$ regardless of F_{fine}, as the fines are unable to completely fit within the voids. For samples with $F_{fine} = 20\%$ and $\chi \geq 6$, $\alpha \approx 0$ and the fines are completely loose within the voids and play almost no role in stress transfer, here $F_{fine} < S^*$.

For the samples at $F_{fine} = 25\%$, which is just above the critical fines content S*, α reduces steeply with increasing χ. At low χ values the fines interact with the coarse particles to a greater degree and therefore are more likely to participate in stress transfer.

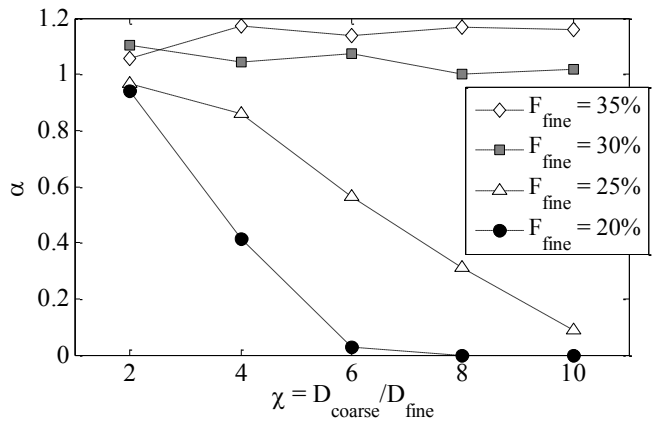

Figure 7: Variation of α with size-ratio

At higher χ values, fines carry reduced effective stress, probably because the interconnected coarse particles dominate the stress transfer, shown by $Z^{coarse\text{-}coarse} > 4$ (Fig. 6(c)). This leaves the fines, which just fill the voids, under a relatively low stress. However, it is worth emphasizing that although these fines are under low stress, they still perform an important supporting role to the more highly stressed particles and their removal, for example due to internal instability under seepage, could lead to the collapse of the stress transferring matrix (Shire et al., 2014, Tordesillas et al., 2009). The role of fines in strong force chains

Thornton and Antony (1998) showed that columns or chains of "strong" contact forces (i.e. forces of above average magnitude) transfer almost all the deviatoric load through granular materials. It is therefore reasonable to take the probability of a fine particle forming part of a strong force chain, $P(strong)_{fine}$ as an indicator of the contribution of the fines to the shear resistance of a sample. $P(strong)_{fine}$ is similar to the concept of the *b* parameter proposed by Thevanayagam et al. (2002) (Equation 3). Note that all the simulations carried out here are under isotropic stress, so it is not possible to determine the role that fines play in deviatoric stress transfer or shear resistance, although this is possible using DEM.

The variation of $P(strong)_{fine}$ with χ is shown in Figure 8. The pattern is similar to the relationship between α, χ and F_{fine} presented in Figure 7, where for $F_{fine} \geq 30\%$ $P(strong)_{fine} > 0.5$ and therefore fines play a significant role in supporting the fabric of the samples, whereas for samples with $F_{fine} \leq 25\%$ $P(strong)_{fine}$ reduces with increasing χ, as the fines are able to fit more efficiently in the voids and so are less likely to interact with the coarse particles which dominate the strong force chains (for each sample the probability of a coarse particle forming a strong force chain is greater than 80%).

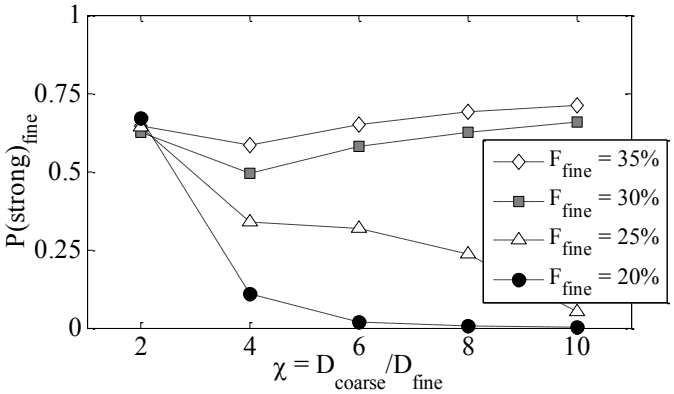

Figure 8: Variation of probability of particle forming part of strong force chain with size ratio

This supports the hypothesis of Rahman et al. (2008) that the role which cohesionless fines play in stress transfer diminishes with both χ and F_{fine} when $F_{fine} < F_{th}$, a threshold fines content . However, care must be taken in defining this threshold content – when $F_{fine} < S^*$ the role of the fines is primarily dependent on χ, and when $F_{fine} > S_{max}$ the coarse and fine play

approximately equal roles. However, for $S^* < F_{fine} < S_{max}$ the role of fines is dependent on both χ and F_{fine}. An added complication is also that the values of S^* and S_{max} are density-dependent (Shire et al., 2014).

4 CONCLUSIONS

This paper presents a series of DEM simulations to investigate the effect of varying the cohesionless fines content and size ratio between coarse and fine particles on the properties of dense bimodal materials. In particular the role of the fines in stress transfer is studied, which is important for the internal stability of soils and the load:deformation response soils with cohesionless fines.

The following conclusions can be drawn from the work:

(a) The minimum void ratio which can be obtained by bimodal samples falls as the size-ratio, $\chi = D_{coarse}/D_{fine}$ increases, in agreement with results presented by Lade et al. (1998).

(b) Micro-scale evidence is shown for two fines contents at which transitions in soil fabric occur: S^*, at which the fines just fill the voids between coarse particles can be seen by increase in the fine coordination number, Z^{fine}. S_{max}, where the fines begin to separate the coarse particles from one another is distinguished by a reduction in the coarse to coarse coordination number to $Z^{coarse\text{-}coarse} < 4$.

(c) Stress-transfer in bimodal samples is highly dependent on fabric, in particular for dense samples it is controlled by χ and F_{fine}. The role of fines in stress transfer can be quantified by the stress-reduction α-factor (Skempton and Brogan, 1994).

(d) At values of $\chi \leq 2$, fine and coarse particles play an approximately equal role in stress transfer ($\alpha \approx 1$), regardless of F_{fine}, as the fines cannot completely fit between the coarse particles.

(e) For $\chi \geq 6$ stress transfer is dependent on both F_{fine} and χ. In particular: *(i)* when $F_{fine} < S^*$ the fines play only a minor role in stress transfer and $\alpha \approx 0$; *(ii)* when $F_{fine} > S_{max}$ the coarse and fine play approximately equal roles and $\alpha \approx 1$; *(iii)* when $S^* < F_{fine} < S_{max}$ an increase in F_{fine} leads to an increase in α, and, when F_{fine} is close to S^*, and increase in χ leads to a reduction in α.

(f) A similar relationship is found between F_{fine}, χ and the probability of a fines forming part of a strong force chain, $P(strong)_{fine}$ as is found between F_{fine}, χ and α.

5 REFERENCES

BEEN, K. & JEFFERIES, M. G. (1985) A State Parameter for Sands. *Géotechnique,* 35**,** 99-112.

CUNDALL, P. A. & STRACK, O. D. L. (1979) A discrete numerical model for granular assemblies. *Géotechnique,* 29**,** 47-65.

ICOLD (2013) *Bulletin on internal erosion of dams, dikes and their foundations: Volume 1:*

KENNEY, T. C. & LAU, D. (1985) Internal Stability of Granular Filters. *Canadian Geotechnical Journal,* 22**,** 215-225.

KÉZDI, Á. (1979) *Soil physics : selected topics,* Elsevier.

LADE, P. V., LIGGIO, C. D. & YAMAMURO, J. A. (1998) Effects of non-plastic fines on minimum and maximum void ratios of sand. *ASTM geotechnical testing journal,* 21**,** 336-347.

LI, M. & FANNIN, R. J. (2012) A theoretical envelope for internal instability of cohesionless soil. *Géotechnique,* 62**,** 77-80.

MCGEARY, R. K. (1961) Mechanical packing of spherical particles. *Journal of the American Ceramic Society,* 44**,** 513-522.

MINH, N. H. & CHENG, Y. P. (2013) A DEM investigation of the effect of particle-size distribution on one-dimensional compression. *Géotechnique,* 63**,** 44-53.

MITCHELL, J. K. (1976) *Fundamentals of soil behavior,* First edition. Wiley.

NI, Q., TAN, T. S., DASARI, G. R. & HIGHT, D. W. (2004) Contribution of fines to the compressive strength of mixed soils. *Géotechnique,* 54**,** 561-569.

PLIMPTON, S. (1995) Fast Parallel Algorithms for Short-Range Molecular-Dynamics. *Journal of Computational Physics,* 117**,** 1-19.

POTYONDY, D. O. & CUNDALL, P. A. (2004) A bonded-particle model for rock. *International Journal of Rock Mechanics and Mining Sciences,* 41**,** 1329-1364.

RAHMAN, M. M., LO, S. R. & GNANENDRAN, C. T. (2008) On equivalent granular void ratio and steady state behaviour of loose sand with fines. *Canadian Geotechnical Journal,* 45**,** 1439-1456.

SHIRE, T. (2014) Micro-scale modelling of granular filters. PhD, Imperial College London.

SHIRE, T. & O'SULLIVAN, C. (2013) Micromechanical assessment of an internal stability criterion. *Acta Geotechnica,* 8**,** 81-90.

SHIRE, T., O'SULLIVAN, C., HANLEY, K. & FANNIN, R. J. (2014) Fabric and effective stress distribution in internally unstable soils. *Journal of Geotechnical and Geoenvironmental Engineering,* Submitted for publication.

THEVANAYAGAM, S., SHENTHAN, T., MOHAN, S. & LIANG, J. (2002) Undrained fragility of clean sands, silty sands, and sandy silts. *Journal of geotechnical and geoenvironmental engineering,* 128**,** 849-859.

THORNTON, C. & ANTONY, S. J. (1998) Quasi-static deformation of particulate media. *Philosophical Transactions of the Royal Society a-Mathematical Physical and Engineering Sciences,* 356**,** 2763-2782.

TORDESILLAS, A., ZHANG, J. & BEHRINGER, R. (2009) Buckling force chains in dense granular assemblies: physical and numerical experiments. *Geomechanics and Geoengineering: An International Journal,* 4**,** 3-16.